Analysis of time-lapse difference AVO with the Pouce Coupe field data

Shahin Jabbari, David D'Amico, Jeff Grossman, Brian H. Russell, Helen Isaac, and Kris Innanen

ABSTRACT

Time-lapse seismology is a cost-effective approach for monitoring the changes in the fluid saturation and pressure over a period of time in a reservoir, in which multiple seismic surveys are done at different time intervals and then compared to see reservoir changes. A multicomponent time-lapse seismic data set was acquired during hydraulic fracturing of two horizontal wells in the unconventional Montney Reservoir at Pouce Coupe Field in the Peace River area by Talisman Energy Inc. In this study, we analyze this data to validate derived linear and nonlinear theoretical results for the time-lapse amplitude versus offset (AVO) difference during the change in a reservoir from the Baseline survey relative to the Monitor survey. We first generate the well tie to determine the location of the reservoir on the seismic data at the Montney Formation. Synthetic logs for P- and S- wave velocities and density are then generated for the Monitor survey. Analyzing these data set at the Baseline and Monitor surveys shows that the linear approximation is good enough to estimate time-lapse AVO difference. This is consistent with the fact that the Pouce Coupe data set has a low Baseline contrast between the cap rock and reservoir and a low time-lapse contrast from the Baseline survey to the time of the Monitor survey. The upper layer of the Montney Formation or the Doig, with a larger Baseline contrast, is also analyzed to evaluate the theoretical results.

INTRODUCTION

The employment of enhanced oil recovery (EOR) techniques affects reservoir properties such as fluid flow and pressure. A time-lapse seismic survey allows us to monitor the production of hydrocarbons by measuring the changes in the behavior of a reservoir over time. Comparison of repeated seismic surveys over months, years, or decades adds a fourth dimension, calendar time, to the seismic data. In a time-lapse seismic survey the Baseline survey, which is acquired prior to production of a reservoir, is compared to the Monitor survey, acquired after a particular interval of time following several geological-geophysical reservoir changes. The difference between the Baseline survey and subsequent Monitor surveys can be analyzed to interpret changes in the reservoir (Greaves and Fulp, 1987; Lumley, 2001; Landrø, 2001). Perturbation (scattering) theory and amplitude variation with offset (AVO) methods can be used to model and invert the difference data in a time-lapse survey. The Baseline survey describes the background medium against which we measure the perturbation detected in the Monitor survey. The perturbation quantifies the changes in P-wave and S-wave velocities and density between the times of the Baseline and Monitor surveys (Stolt and Weglein, 2012; Innanen et al., 2014).

Jabbari et al. (2015) formulate a framework to model linear and nonlinear elastic time-lapse difference AVO ($\Delta R_{PP}(\theta)$, where θ is the incident angle) for P-P sections using perturbation theory. This framework consist of a series expansion for the difference re-
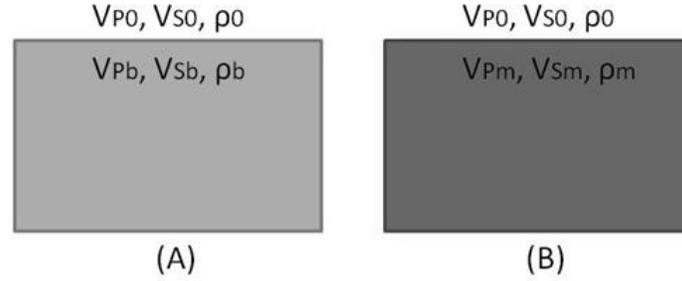
FIG. 1. Rock properties of the model at the time of the Baseline (A) and Monitor (B) survey.

flection coefficient $\Delta R_{PP}(\theta)$ in orders of (1) $\sin^2 \theta$, (2) elastic property contrasts across the reflector (e.g., caprock over reservoir) at the time of the Baseline survey, and (3) elastic property time-lapse perturbation (Jabbari et al., 2015). To first order the resultant $\Delta R_{PP}(\theta)$ is in agreement with the result obtained by Landrø (2001). The higher order terms provide corrections when contrasts are large. Jabbari et al. (2015) in the second part of their study, validate the linear and nonlinear $\Delta R_{PP}(\theta)$ modeling terms using physical modeling data acquired at the CREWES/University of Calgary facility.

In the present study, in conjunction with Talisman Energy Inc., the Pouce Coupe time-lapse data set, is used to validate the theoretical linear and nonlinear time-lapse AVO difference derived by Jabbari et al. (2015). This time-lapse data set was acquired during hydraulic fracture stimulations of two horizontal wells in the Montney at the Pouce Coupe Field, Alberta, Canada.

Theory

Our time-lapse survey consists of two seismic experiments; a Baseline survey followed by a Monitor survey. The P-wave and S-wave velocities and the density change from the time of the Baseline survey relative to the Monitor survey. This pair of models shown in Figure 1 is consistent with an unchanging cap rock overlying a porous target which is being produced. Let V_{P_0}, V_{S_0}, ρ_0 and V_{P_b}, V_{S_b}, ρ_b be the rock properties of the cap rock and reservoir at the time of Baseline survey. Setting boundary conditions in the problem leads to Zoeppritz equations which can be rearranged in a matrix form (Keys, 1989; Aki and Richards, 2002). The reflection coefficients for the Baseline and Monitor surveys can then be determined from the Zoeppritz equations by using Cramer's rule and forming auxiliary matrices. For the Monitor survey, rock properties for cap rock are the same, but reservoir properties change to V_{P_m}, V_{S_m}, ρ_m. The reflection coefficient difference between the Baseline and Monitor surveys is then calculated as:

$$\Delta R_{PP}(\theta) = R_{PP}^m(\theta) - R_{PP}^b(\theta) \tag{1}$$

In our time-lapse study we have consider two groups of perturbation parameters, using the scattering nomenclature found in Stolt and Weglein (2012). The first group expresses the perturbation caused by propagating the wavefield from the first medium to the second

medium in the Baseline survey:

$$b_{VP} = 1 - \frac{V_{P_0}^2}{V_{P_b}^2}, \quad b_{VS} = 1 - \frac{V_{S_0}^2}{V_{S_b}^2}, \quad b_\rho = 1 - \frac{\rho_0}{\rho_b}. \tag{2}$$

The second group expresses the time-lapse perturbation and accounts for the changes in the Monitor survey relative to the Baseline survey.

$$a_{VP} = 1 - \frac{V_{P_b}^2}{V_{P_m}^2}, \quad a_{VS} = 1 - \frac{V_{S_b}^2}{V_{S_m}^2}, \quad a_\rho = 1 - \frac{\rho_b}{\rho_m}. \tag{3}$$

$\Delta R_{PP}(\theta)$ is calculated and then expanded in first and second order for all six perturbations given equations 2 and 3, and $\sin^2 \theta$.

$$\Delta R_{PP}(\theta) = \Delta R_{PP}^{(1)}(\theta) + \Delta R_{PP}^{(2)}(\theta) + \Delta R_{PP}^{(3)}(\theta) + ... \tag{4}$$

The linear and second order terms in the reflection coefficient difference are as follows (Jabbari et al., 2015):

$$\Delta R_{PP}^{(1)}(\theta) = \left[\frac{1}{4} + \frac{1}{4}\sin^2\theta\right] a_{VP} + \left[-2\left(\frac{V_{S_0}}{V_{P_0}}\right)^2 \sin^2\theta\right] a_{VS} + \left[\frac{1}{2} - 2\left(\frac{V_{S_0}}{V_{P_0}}\right)^2 \sin^2\theta\right] a_\rho$$

$$\Delta R_{PP}^{(2)}(\theta) = \left[\frac{1}{8} + \frac{1}{4}\sin^2\theta\right] a_{VP}^2 + \left[\left(\frac{V_{S_0}}{V_{P_0}}\right)^3 \sin^2\theta - 2\left(\frac{V_{S_0}}{V_{P_0}}\right)^2 \sin^2\theta\right] a_{VS}^2$$

$$+ \left[\frac{1}{4} - \frac{1}{4}\left(\frac{V_{S_0}}{V_{P_0}}\right)\sin^2\theta - \left(\frac{V_{S_0}}{V_{P_0}}\right)^2 \sin^2\theta + \left(\frac{V_{S_0}}{V_{P_0}}\right)^3 \sin^2\theta\right] a_\rho^2$$

$$+ \left[2\left(\frac{V_{S_0}}{V_{P_0}}\right)^3 \sin^2\theta - \left(\frac{V_{S_0}}{V_{P_0}}\right)^2 \sin^2\theta\right] a_\rho a_{VS}$$

$$+ \left[2\left(\frac{V_{S_0}}{V_{P_0}}\right)^3 \sin^2\theta - 2\left(\frac{V_{S_0}}{V_{P_0}}\right)^2 \sin^2\theta\right] a_{VS} b_{VS}$$

$$+ \left[\frac{1}{4}\sin^2\theta\right] a_{VP} b_{VP} + \left[2\left(\frac{V_{S_0}}{V_{P_0}}\right)^3 \sin^2\theta - \left(\frac{V_{S_0}}{V_{P_0}}\right)^2 \sin^2\theta\right] b_\rho a_{VS}$$

$$+ \left[2\left(\frac{V_{S_0}}{V_{P_0}}\right)^3 \sin^2\theta - \left(\frac{V_{S_0}}{V_{P_0}}\right)^2 \sin^2\theta\right] a_\rho b_{VS}$$

$$+ \left[2\left(\frac{V_{S_0}}{V_{P_0}}\right)^3 \sin^2\theta - \frac{1}{2}\left(\frac{V_{S_0}}{V_{P_0}}\right)\sin^2\theta\right] b_\rho a_\rho \tag{5}$$

More details, including the third order terms, can be found in Jabbari et al. (2015).

Pouce Coupe time-lapse multicomponent seismic data

4D time-lapse, multicomponent seismic surveys were acquired by Talisman Energy Inc. at the Pouce Coupe Field, which is located on the border between Alberta and British

TRIASSIC TABLE OF FORMATIONS, PEACE RIVER ARCH

PERIOD	EPOCH	AGE	OUTCROP		BC - OGC		TALISMAN BC		AB - EUB
TRIASSIC	LATE	Carnian	Luddington	Charlie Lake	Schooler Creek	Charlie Lake	Charlie Lake	Artex	Charlie Lake
	MIDDLE	Ladinian/ Anisian	Liard		Daiber	Halfway	Halfway	Upper Middle Lower	Halfway
						Doig	Doig	Upper	Doig
								Middle	
								Lower (PO4)	
							Montney	F	
	EARLY	Spathian	Toad	Vega-Phospho		Montney		E	
		Smithian						D	Montney
								C	
		Dienerian/ Griesbachian	Grayling					B	
PERMIAN			PERMIAN		BELLOY		BELLOY		BELLOY

FIG. 2. Triassic Montney Formation in the Peace River Arch region. Pouce Coupe Field is represented by the colored Formations in the Repsol BC chart section (courtesy of Repsol S.A.).

Columbia in the Peace River area . The target Formation in these seismic acquisitions was the Triassic Montney Siltstone reservoir (Figure 2).

The Montney Formation is composed of fine-grained, pseudo-turbidites proximal to shoreface deposition and is classified as an organic-rich argillaceous siltstone and sandstone package. Information obtained by Talisman Energy Inc. reports the Montney reservoir to have a matrix permeability of 0.01-.02 mD and porosity of 6-10 % within the Pouce Coupe Field. The unconventional Montney reservoir at Pouce Coupe contains tight gas siltstones and sandstones and produces both gas and liquid hydrocarbons. For economic production, enhanced permeability pathways of natural and induced fractures are required due to the tight nature of the Montney (Davies et al., 1997; Davey, 2012). The Montney Formation is subdivided, from its base, into units A, B, C, D, E and F. The Formation is overlain by the Doig Phosphate and underlain by the Permian Belloy (Figure 3).

The Baseline survey, acquired in March 2008, was recorded after completion and stimulation of the 100/07-07 well, but before production was initiated. The first Monitor was acquired from December 8 to 10, 2008, after 8 months of Montney gas production from the 100/07-07 well. The purpose of acquiring this survey was to characterize the reservoir condition prior to hydraulically fracturing the two horizontal wells. The hydraulic fracture operations took place in two separate stages on the two horizontal wells, and another two subsequent Monitor surveys were acquired after each fracture event. Monitor 2 and 3 were acquired between December 13-14, after fracturing the horizontal well 100-02-07 (targeting the Lower Montney unit C) and between December 18-19, after fracturing the horizontal well 100-07-07 (targeting the lower Upper Montney unit D), respectively, as in Figure 4 (Atkinson, 2010; Atkinson and Davis, 2011).

Seismic data were recorded by CGGVeritas on a patch grid of about 5 km^2 (Figure 5).
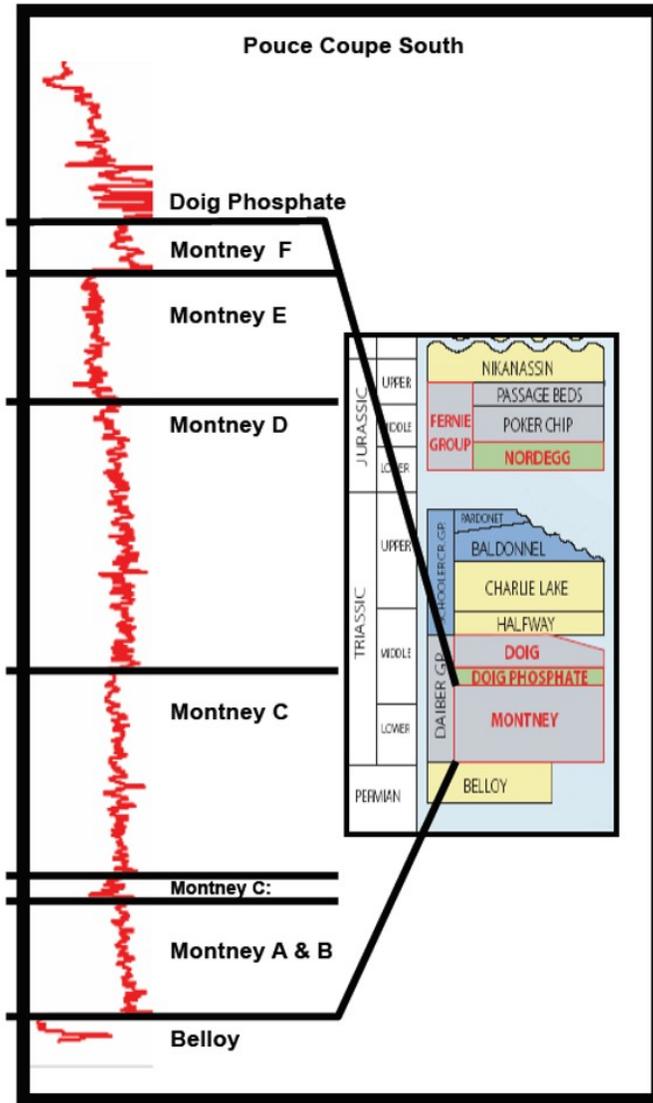
FIG. 3. Type log of the Triassic Montney in the southern Pouce Coupe Field. Red curve is the gamma ray (Steinhoff, 2013).
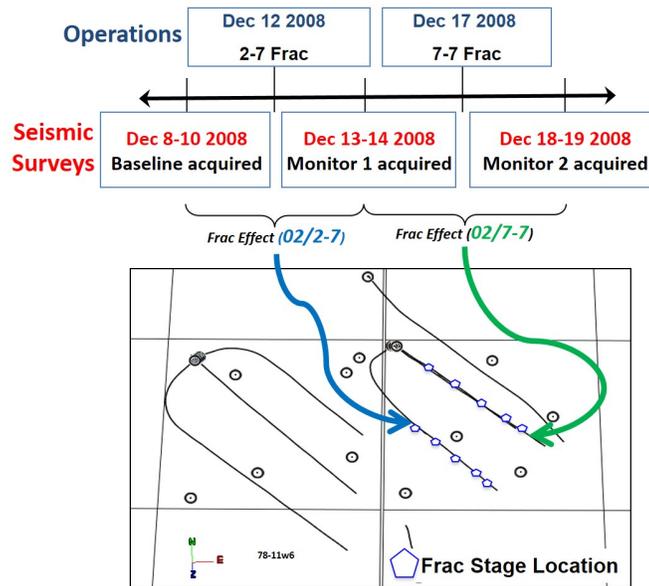
FIG. 4. Pouce Coupe time-lapse seismic and field operations timeline. The map shows two horizontal wells hydraulically stimulated (2-07 well and 7-07 well) and the location of the vertical shear sonic log (13-12 well). Modified from Atkinson (2010).
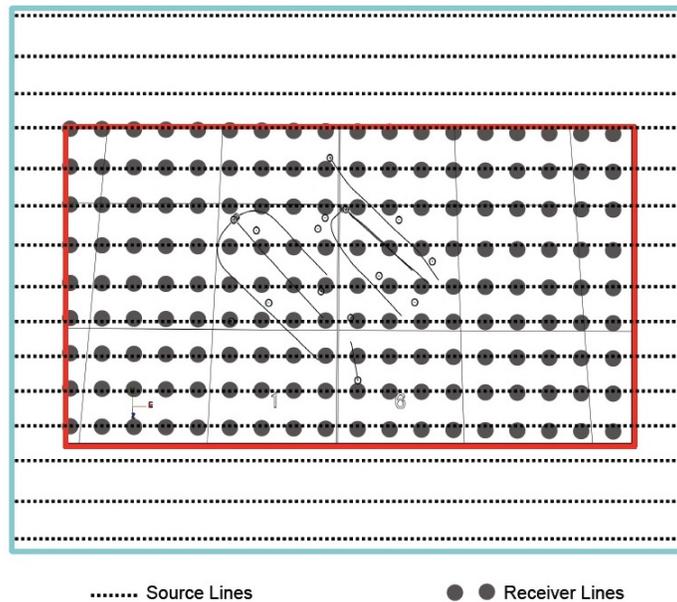

FIG. 5. Pouce Coupe time-lapse, multicomponent seismic survey acquisition layout. The resulting 1.6 km × 3 km patch is centered over horizontal wells 2-07 and 7-07. Modified from Atkinson (2010).
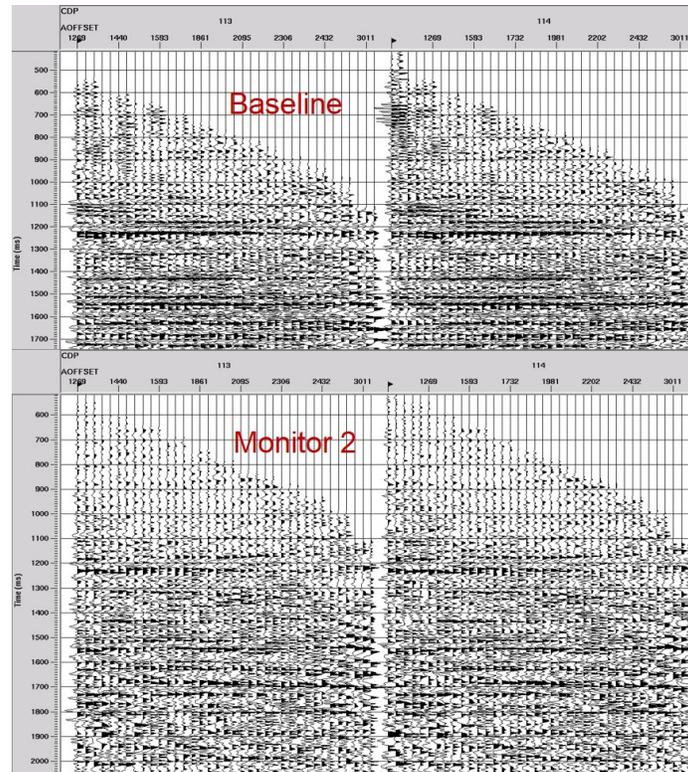
FIG. 6. PSTM (Pre stack time migration) CDP (common depth point) gathers for the Baseline and The Monitor 2 surveys.

The survey grid consists of 144 buried 3C receivers and 1241 shot holes forming a field layout of 41 inlines and 101 crosslines. The bin size is 50 m × 100 m (the patch is twice bigger in E-W direction). The recording length was 6 seconds with a sampling interval of 2 ms. A result of the survey design was uniform $360°$ azimuth for different offset distribution which provides data for future AVO/AVAZ analysis. The processing was completed by Sensor Geophysical Ltd. in July, 2013. The processing flow includes statics correction, prestack noise attenuation, surface consistent deconvolution, CMP (common mid point) stacking, FK (frequency enhancement) filter, radon multiple and 2-term normal moveout. Subsequently, Sensor Geophysical Ltd reprocessed the data making use of a set of new methods to enhance time-lapse repeatability and improve prestack shear wave splitting analysis. Receiver Azimuth Detection and Rotation (RADAR) was utilized to detect and correct receiver azimuths, and this improved the quality of the subsequent steps of processing the horizontal receiver components (Grossman et al., 2013; Steinhoff, 2013). Further details of multicomponent processing are outlined in Steinhoff (2013).

The multicomponent surface seismic data set in Pouce Coupe includes a Baseline survey with two subsequent Monitor surveys. The acquisition was designed to cover a full 360 degree azimuth and offset range from 340 to 3011 meters to a bin size of 50 m by 50 m. Figure 6 shows prestack time migration common depth points (CDP) gathers for the Baseline and Monitor 2.
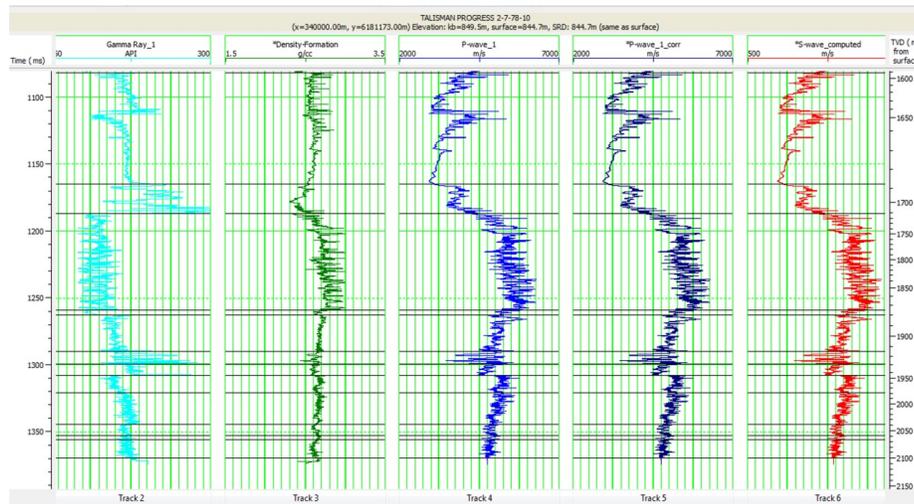
FIG. 7. Gamma, P-wave, S-wave, and density logs for the horizontal well 102-02-07-078-10W6

Methodology

To correlate seismic character to subsurface geology and estimate the location of the horizons on the seismic sections, a synthetic seismogram was generated using a wavelet extracted from the horizontal well, 102-02-07-078-10W6, and reflectivity derived from P-wave sonic and density logs. The S-wave log is calculated using Castagna's Equation with parameters of $V_S = 0.8619V_P - 1172$ m/s. Figure 7 shows different logs obtained by 102-02-07-078-10W6 well including the computed S-wave log and edited or corrected P-wave log used for the synthetic seismogram generation.

This synthetic seismic trace is aligned to the seismic section at the well location to relate horizon tops with specific reflections on the seismic section. Figure 8 shows the resultant well tie aligned with the Baseline seismic section which allows us to correlate the Montney Formation to the seismic. From this estimation, amplitude versus offset analysis can be obtained.

The Baseline seismic was interpreted using the generated synthetic trace. The synthetic trace has been used to estimate the depth of different horizons, specially the target horizon, the tops of Montney C and D (Figure 9). The same method can be used to interpret the seismic data for the Monitor seismic sections. But prior to this, we need to derive log information at the time of the Monitor surveys, as well logs were not acquired at the time of Monitor surveys. All log data were acquired at the time of the Baseline survey and before inducing the fractures. The synthetic logs for the Monitor survey are modeled by modeling the parameters in the systematic changes during the fracture operations. The input parameters include initial P-wave, S-wave, and density logs at the time of the Baseline survey, reservoir parameters such as water saturation, gas saturation, temperature, pressure, salinity, and matrix before and after the fracture operations. Figure 10 shows the synthetic sonic log aligned on the Monitor seismic section.

Perturbation parameters in equation 3 and equation 4 should be calculated in order to
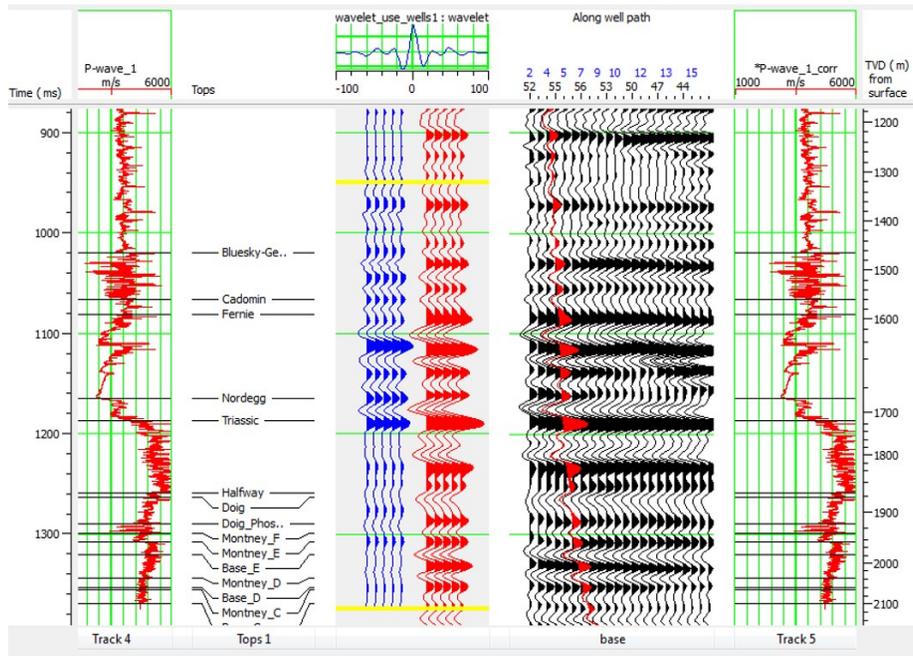
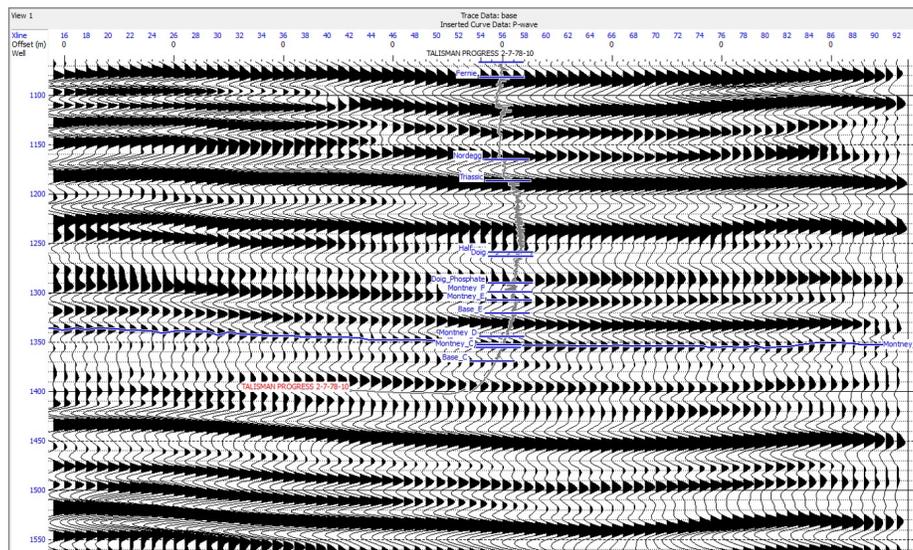FIG. 8. Vertical well tie with Baseline P-wave seismic.

FIG. 9. Estimating the horizon times on the seismic section by tying synthetic in Figure 8 to the Baseline seismic data.
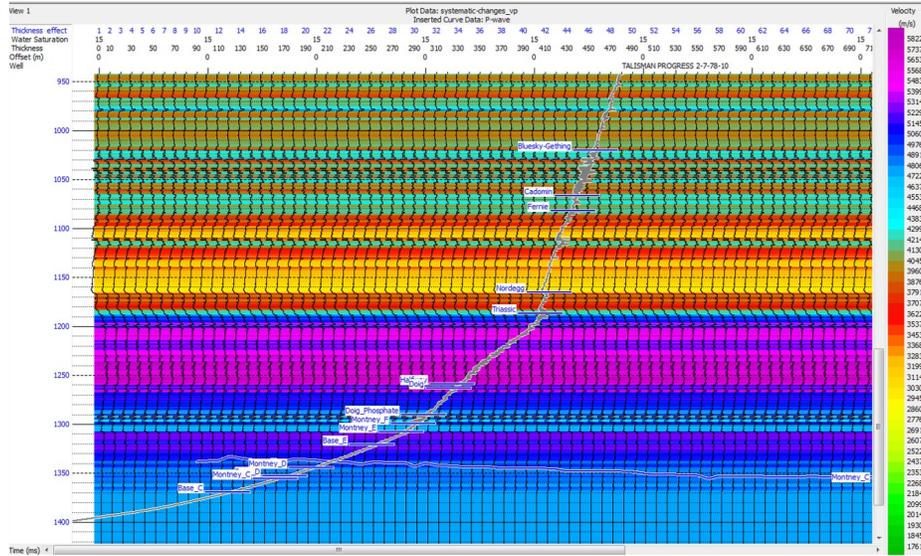
FIG. 10. Synthetic P-wave log representing post-fracture condition created using systematic changes in Hampson Russell

derive the reflection coefficient for time-lapse difference data or $\Delta R_{PP}(\theta)$. This is possible if we have the P- and S-wave velocities, and density information for the cap rock (layer just above the reservoir), and reservoir at the time of the Baseline and Monitor surveys. The top of the Montney C and the top of the Montney D are the interfaces between the cap rock and the reservoir. V_{P_0}, V_{S_0}, ρ_0 and V_{P_b}, V_{S_b}, ρ_b are derived from the well logs obtained at the time of the Baseline survey. We used synthetic logs at the time of the Monitor survey to estimate V_{P_m}, V_{S_m}, ρ_m after the fracture operations (Figure 10).

Results

With three sets of the P-, S- wave velocities, and the density for the Formation above the reservoir or target, and the reservoir itself before and after the fracture, exact $\Delta R_{PP}(\theta)$ for the Baseline, Monitor, and their difference are calculated using the Zoeppritz equations (Figure 11). The red curve representing the time-lapse difference reflection coefficient is almost at zero for all offsets. The reason is because the reflection coefficient, R_{PP}, for the Baseline and Monitor surveys are almost identical. This can be expected by investigating the well log information and seismic sections (as in Figure 8 -10) at the interface of the tops of Montney C and Montney D (as the productive layers or reservoir layers). Investigating the difference in gamma, P-, S- wave, and density logs in Figure 7 in the area of interest at around 1350 ms time depth, we can see the low Baseline contrast between the reservoir (Montney C) and the cap rock (layer above it by our definition). Also the seismic parameters, P-, S- wave velocities, and density for the reservoir Formation at the time of the Baseline survey relative to the Monitor survey are similar. This explains the similarity of reflection coefficient for the Baseline and Monitor surveys. Choosing another interface such as the base of the Doig or the base of the Montney E gives a higher contrast in the Baseline survey.

In figure 12, the exact difference data are compared to the linear and nonlinear time-
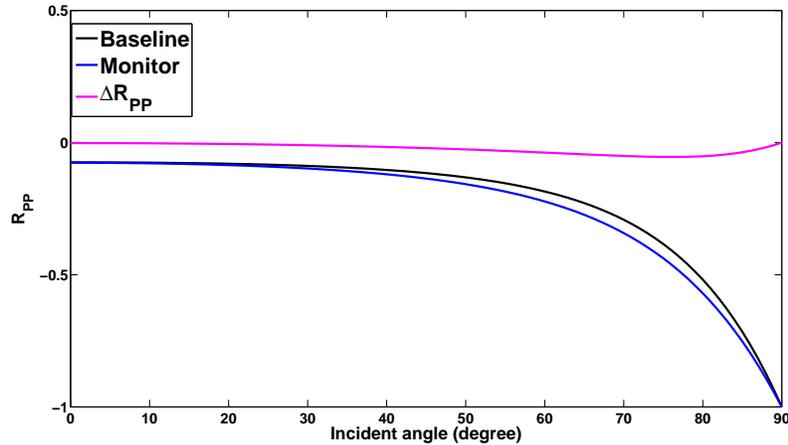
FIG. 11. $R_{PP}(\theta)$ for the Baseline (black) and Monitor (blue) surveys and for their difference (red), $\Delta R_{PP}(\theta)$, for Pouce Coupe data set
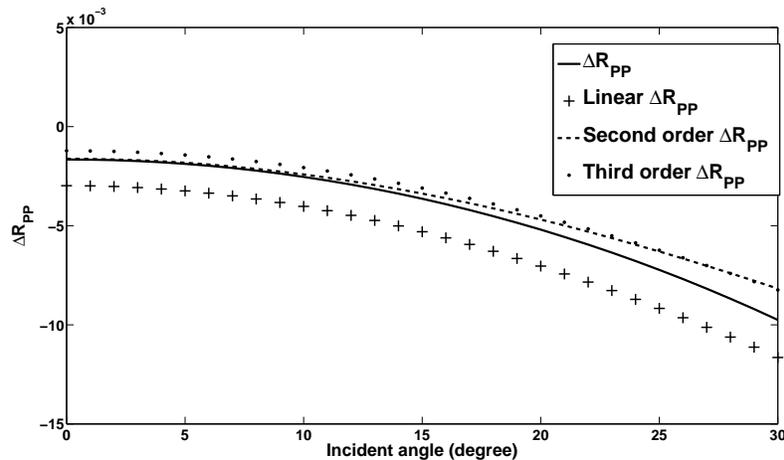

FIG. 12. $\Delta R_{PP}(\theta)$ for the exact (solid line), linear (+++), second (—), and third order (...) approximation for Pouce Coupe data set

lapse AVO approximation derived from the results of Jabbari et al. (2015) (equation 5). These results shows that higher order approximations in $\Delta R_{PP}(\theta)$ can estimate the difference data with slightly more accuracy.

CONCLUSIONS

Changes in fluid saturation and pressure, which have an impact on elastic parameters, such as P-wave and S-wave velocities and density, can be approximated by applying time-lapse AVO analysis methods. An increase in pore pressure has been induced following hydraulic fracture operations in the unconventional Montney shale reservoir. This will affect seismic parameters including the compressional wave velocity. Due to the tight nature and low permeability of the Montney reservoir, the injection of fluid into the reservoir during the fracture operations will affect only close vicinity to the fractures. For this reason, the change in P-wave velocity has to be investigated in the close vicinity to the hydraulic

fractures in the horizontal wells to be able to detect a significant seismic signature. This is practically impossible with the present Pouce Coupe data set.

Jabbari et al. (2015) concluded that the higher order terms in time-lapse AVO represent corrections appropriate for large P-wave and S-wave velocity and density contrasts in the reservoir from the time of the Baseline survey to the time of the Monitor survey. They also showed that time-lapse AVO difference data are function of both Baseline interface properties and time-lapse changes.

The Pouce Coupe data set shows low contrast between the cap rock and reservoir in the Baseline survey and also lower contrast in time-lapse changes from time of the Baseline survey relative to the time of the Monitor survey. Therefore, linear approximation is good enough to approximate time-lapse difference for the Pouce Coupe data set for Montney C or Montney D layers as the reservoir interfaces. Because of the small time-lapse contrast, this data set is not an appropriate data set which can be used to evaluate the nonlinearity of time-lapse difference AVO results. The same analysis can be applied to another interface with a larger seismic signature in the Baseline survey such as the Doig or the upper layers of Montney Formation.

ACKNOWLEDGMENTS

REFERENCES

Aki, K., and Richards, P. G., 2002, Quantitative Seismology: University Science Books, 2 edn.

Atkinson, J., 2010, Multicomponent time-lapse monitoring of two hydraulic fracture stimulations in an unconventional reservoir, Pouce Coupe Field, Canada: M.Sc. thesis, Colorado School of Mines.

Atkinson, J., and Davis, T., 2011, Multi-component time-lapse monitoring of two hydraulic fracture stimulations in the Pouce Coupe Field unconventional reservoir, **29**, No. 10, 91–97.

Davey, H., 2012, Geomechanical characterization of the Montney shale Northwest Alberta and Northeast British Columbia: M.Sc. thesis, Colorado School of Mines.

Davies, G., Moslow, T., and Sherwin, M., 1997, The lower triassic montney, west-central alberta.: Bulletin of Canadian Petroleum Geology, **45**, No. 4, 474–505.

Greaves, R. J., and Fulp, T., 1987, Three-dimensional seismic monitoring of an enhanced oil recovery process: Geophysics, **52**, No. 9, 1175–1187.

Grossman, J., Popov, G., and Steinhoff, C., 2013, Integration of multicomponent time-lapse processing and interpretation: Focus on shear-wave splitting analysis: The Leading Edge, **32**, No. 1, 32–38.

Innanen, K. A., Naghizadeh, M., and Kaplan, S. T., 2014, Perturbation methods for two special cases of the time-lapse seismic inverse problem: Geophysical Prospecting, **62**, 453–474.

Jabbari, S., Wong, J., and Innanen, K. A., 2015, A theoretical and physical modeling analysis of the coupling between baseline elastic properties and time-lapse changes in determining difference amplitude variation with offse: Geophysics, **80**, No. 6, 50–53.

Keys, R. G., 1989, Polarity reversals in reflections from layered media: Geophysics, **54**, 900–905.

Landrø, M., 2001, Discrimination between pressure and fluid saturation changes from time-lapse seismic data: Geophysics, **66**, No. 3, 836–844.

Lumley, D. E., 2001, Time-lapse seismic reservoir monitoring: Geophysics, **66**, No. 1, 50–53.

Steinhoff, C., 2013, Multicomponent seismic monitoring of the effective stimulated volume associated with hydraulic fracture stimulations in a shale reservoir, Pouce Coupe Field, Alberta, Canada: M.Sc. thesis, Colorado School of Mines.

Stolt, R. H., and Weglein, A. B., 2012, Seismic Imaging and Inversion: Volume 1: Application of Linear Inverse Theory: Cambridge University Press.